

Phase behavior of mixtures of oppositely charged protein nanoparticles at asymmetric charge ratios

P. Maarten Biesheuvel,^{1,2} Saskia Lindhoud,¹ Martien A. Cohen Stuart,¹ and Renko de Vries¹

¹Laboratory of Physical Chemistry and Colloid Science, Wageningen University, Dreijenplein 6, 6703 HB Wageningen, The Netherlands

²Max Planck Institute for Colloids and Surfaces, Am Mühlenberg 1, 14476 Potsdam, Germany

(Received 20 January 2006; published 25 April 2006)

We present experimental and theoretical results for the phase behavior of mixtures of oppositely charged globular protein molecules in aqueous solutions containing monovalent salt. These colloidal mixtures are interesting model systems, on the one hand for electrolyte solutions (“colloidal ionic liquids”), and on the other for mixtures of oppositely charged (bio)macromolecules, colloids, micelles, etc., with the range of the electrostatic interactions (Debye length) easily tunable from much smaller to much larger than the particle size, simply by adding different amounts of monovalent salt. In this paper we investigate the phase behavior of such mixtures in the case that equally sized colloids have a large difference in charge magnitude. This is possible at any mixing ratio because small ions compensate any colloidal charge asymmetry. Our experimental system is based on lysozyme, a positively charged “hard” globular protein molecule, and succinylated lysozyme, a chemical modification of lysozyme which is negatively charged. By changing the solution pH we can adjust the ratio of charge between the two molecules. To describe phase separation into a dilute phase and a dense “complex” phase, a thermodynamic model is set up in which we combine the Carnahan–Starling–van der Waals equation of state with a heterogeneous Poisson–Boltzmann cell model and include the possibility that protein molecules adjust their charge when they move from one phase to the other (charge regulation). The theory uses the nonelectrostatic attraction strength as the only adjustable parameter and reasonably well reproduces the data in that complexation is only possible at intermediate pH , not too asymmetric mixing ratios, and low enough ionic strength and temperature.

DOI: [10.1103/PhysRevE.73.041408](https://doi.org/10.1103/PhysRevE.73.041408)

PACS number(s): 82.70.Dd, 82.35.Rs, 87.14.Ee

INTRODUCTION

Complexation of oppositely charged macroions, such as micelles, polyelectrolytes, and/or colloids is observed in a large range of biological systems, and is exploited in many technologies such as microencapsulation by complex coacervates, soluble DNA-polycation complexes for nonviral gene transfer, and thin film fabrication by layer-by-layer deposition of oppositely charged polyelectrolytes.

Because of the combination of a repulsion between like-charged particles and an attraction between oppositely charged particles, these systems show very interesting phase behavior (“associative phase separation”) where both soluble as well as macroscopic “complex” phases can be observed when the attractive electrostatic forces are strong enough. Compared to systems involving charged polymer chains, relatively little attention has been paid to systems involving oppositely charged spherical particles, such as proteins and colloids. Nevertheless, such systems are interesting both as model systems, and because of possible technological and scientific implications [1–3]. For example, Leunissen *et al.* [4] recently showed how to exploit electrostatic complexation to assemble various novel colloidal cocrystals with particles differing in both charge and size. Furthermore, the cytosol of living cells may be viewed as a mixture of proteins of different charge (sign). Recently it was suggested that, at least for prokaryotes, the cytoplasm is quite close to the phase boundary for macroscopic phase separation [5]. Complexation of the minority of basic proteins with acidic globular proteins may contribute significantly to the stability or instability of the cytoplasm.

To study phase behavior in such mixtures, simple experimental model systems are required. Ideally these are based on spherical particles, homogeneously charged, and with the range and strength of the interaction forces easily tunable. For equilibrium structures to be formed, the range of the attraction should be of the order of the particle radius or larger. To that end, Leunissen *et al.* [4] and Bartlett and Campbell [6] who use polymethyl methacrylate PMMA particles of a radius of $\sim 1 \mu\text{m}$, work in highly deionized solvents of a Debye length κ^{-1} of ~ 0.2 to $1.6 \mu\text{m}$. Raşa *et al.* [7] use particles that are of the order of 10^2 smaller (size $\sim 15 \text{ nm}$), and by working in ethanol realize a Debye length κ^{-1} of 10 – 20 nm . Our approach [8] is to go to even smaller “colloidal ions” by using globular (approximately spherical) protein molecules, of a radius of $\sim 2 \text{ nm}$. To obtain Debye lengths in the relevant range we can simply work in aqueous solution, and can realize values for $0.2 < \kappa R < 2$ by adding monovalent salt at reasonable values for the ionic strength (1 – 100 mM). By changing pH we can quite easily tune the charge on the colloids, which will be the topic of this report.

In a previous report [8] we introduced our model system which is based on lysozyme, a “hard” globular protein molecule, positively charged for pH below its isoelectric point ($pI \sim 11$), and succinylated lysozyme, a chemical modification of lysozyme which is negatively charged above $pH \sim 4.5$. Because the negative molecule is synthesized from the positive one (by chemically modifying some of the amino acid residues), we believe that to a good approximation the molecules are the same, except for their charge. In Ref. [8] we studied the macroscopic phase behavior of this system at

a pH where the two molecules are about equally charged (in magnitude). In the present paper we will investigate the behavior of this model system at asymmetric charge ratios by bringing the pH toward the isoelectric point of one of the protein molecules.

To describe the experimental observations (either incipient conditions for phase separation, or amount of complexed material), we use a thermodynamic theory developed in Ref. [8] for mixtures of charged spherical colloids that interact across an aqueous solution containing co- and counterions. Other theoretical approaches are described in Ref. [8] while molecular dynamics simulations of mixtures of oppositely charged spheres were made by Liu and Luijten [9] and Caballero *et al.* [10] In the model of Ref. [8] the charge on the colloids was calculated under the condition of infinite dilution, and assumed constant, independent of the presence of nearby colloids. At pH 7–8 this is a very good approximation for the two types of lysozyme molecules, as their charge is (in that pH range) quite independent of local proton concentration and therefore also independent of the proximity to other molecules. However, this is not generally true, certainly not near the isoelectric point where the charge of a protein molecule depends strongly on the local proton concentration. In the present paper we include the possibility that nearby colloids influence the proton concentration near a protein molecule and thus its charge (“charge regulation”). In the thermodynamic functions we must additionally include a chemical term (a contribution that contains the proton adsorption energy, and the entropy of the two states of the amino acid, charged and uncharged). We will compare theoretical results based on the assumption that the protein molecules have the same charge in both phases [constant-charge (CC) model], with the situation that they adjust their charge according to local conditions [i.e., proton concentration; the charge-regulation (CR) model].

In this paper we use for the protein molecules alternatively the terms “particle” and “colloid.” The dense phase is also called the “complex” phase; the term “supernatant” is sometimes used for the dilute phase. In the following sections we describe the thermodynamic theory, the experimental program and results, and the comparison of theory with the data.

THEORY

A theoretical model is described for phase separation in mixtures of oppositely charged protein nanoparticles in aqueous solution. The model is an extension of that described in Ref. [8], by including the ionizable character of the protein molecules in more detail, namely, by considering that the protein charge not only is a function of ionic strength and pH , but also of the density and composition of the respective phase (dilute phase or complex phase), i.e., the proximity to other protein molecules (CR model), because the proton concentration near the protein molecule is modified, and via the proton adsorption reactions the charge is affected. The fixed-charge (or CC) model calculates the protein charge based on a dilute protein solution, that is, when the diffuse layer around the molecule extends undisturbed to infinity, and the

protein charge is influenced only by pH and ionic strength.

Typically, within the complex phase the electrostatic potential at the surface of the protein molecule is closer to zero than in the solution phase; thus, in the CR model both molecules have a higher charge (in magnitude). Therefore, compared to a fixed-charge approach, allowing for charge regulation leads to an increased range in which complexation is thermodynamically possible. Around pH 7.5 (as in Ref. [8]) both molecules have a charge that is rather independent of pH , and assuming a fixed protein charge is a good approximation. However, at pH closer to the isoelectric point a protein molecule becomes more titratable (charge more dependent on local proton concentration), and charge regulation may become important.

Heterogeneous cell model

To describe the electrostatic interactions, we use the heterogeneous Poisson-Boltzmann (PB) cell model of Ref. [11], where it was applied to charge-regulating coil-like polyelectrolytes using a cylindrical geometry without linearizing the PB equation. In Ref. [8] the model was applied to oppositely charged spheres of a fixed charge in the Debye-Hückel (DH) limit. Here, we use the DH limit as well, while we will analyze both the CC and CR models.

In the heterogeneous cell model we consider an envelope of solvent plus small ions around each charged colloid; the envelope plus colloid together constitute one spherical cell. For a bidisperse mixture we consider two types of cells. The PB equation is solved in a spherical geometry within the solvent envelope between colloid and cell edge. The boundary conditions are Gauss’ law at the surface of the colloid, a common value for the electrostatic potential ψ at the edge of all cells, and finally overall electroneutrality of all cells (of the two types) combined, which translates into a relation between the two (different) field strengths at the edge of the (two) different types of cells (and the number concentration of each type of cell). The heterogeneous cell model simplifies to the traditional one-component cell model if only one type of colloid is present, and, for very dilute conditions, results in the classical expression for the potential around a single charged spherical colloid. Compared to a one-component cell model, the field strength at the edge of the cell, however, is no longer set to zero a priori, but is self-consistently obtained from the requirement of overall electroneutrality. Because the magnitude of the electrostatic potential is a measure of the electrostatic repulsion between the colloids, and (the square of) the field strength is a measure of the electrostatic attraction, the protein molecules can electrostatically both attract and repel. This is different from one-component cell models where we always have electrostatic repulsion between the colloids. The cell model has the advantage that it is not necessary to describe the positions of the different colloids relative to one another, which is required when the model is based on binary, or two-body, interaction potentials (such as the Yukawa potential). In the cell model interactions of a given colloid with all other colloids are included via the boundary condition at the edge of the cell.

Because the protein molecules are of equal radius a , it is quite natural to assume in the cell model that the two types of cells have the same outer radius b after which the volume density of all colloids combined, ϕ , is given by

$$\phi = \frac{a^3}{b^3}. \quad (1)$$

We use the Debye-Hückel approximation of linearizing the PB equation to be solved in the spherical, annular, space between the protein molecule surface (at $r=a$) and the edge of the cell ($r=b$), which results for the electrostatic potential $y_{p,i}$ at the surface of the colloid, where $r=a$, in cell i , in

$$y_{p,i} = \frac{\kappa\lambda_B}{t_h + \kappa a} \left(\frac{t_h}{\kappa a} Z_i + (1 - t_h^2) \frac{Q_1}{\phi} \sum_{i=1,2} Z_i \phi_i \right) \quad (2)$$

where

$$Q_1 = \left[1 - \frac{a}{b} - \left(\frac{1}{\kappa b} - \kappa a \right) t_h \right]^{-1}, \quad t_h = \tanh(\kappa b - \kappa a). \quad (3)$$

Here κ is the inverse of the Debye length, given by $\kappa^2 = 8\pi\lambda_B n_\infty$, when all ions are monovalent. The ionic strength n_∞ ($=c_\infty N_{av}$ with c_∞ in mM) is defined in a virtual colloid-free phase containing only the small ions, in equilibrium with the (two) phase(s) containing the colloids (thus, we fix the ion chemical potential as $\ln n_\infty$). N_{av} is Avogadro's number, and λ_B the Bjerrum length (in water $\lambda_B = 0.72$ nm).

The protein charge Z_i is obtained according to the Tanford titration model, which considers a spherical particle with a smeared-out surface charge [8,12–15]. The total protein charge Z_i is given by a summation over the six types of ionizable amino acid groups of number q_i , charge sign z_i , and ionization degree α_i ,

$$Z = \sum_i q_i z_i \alpha_i. \quad (4)$$

The ionization degree α_i of each amino acid residue relates to the electrostatic surface potential y_p according to

$$\alpha_i = \frac{1}{1 + 10^{\bar{z}_i(pH - pK_i)} e^{\bar{z}_i y_p}} \quad (5)$$

where pH is the background pH (a measure of the chemical potential of protons in the system) and pK the intrinsic pK value, a thermodynamic number directly related to the (non-electrostatic) adsorption energy of a proton to a certain amino acid group. Now, whereas in the CC model we calculate the charge on the basis of assuming an infinitely dilute solution, in the CR model we self-consistently relate y_p to Z using the heterogeneous cell model. Typically, this implies that because the potentials y_p are closer to zero in the dense phase than in solution, the charge of both the negative and the positive colloids is higher in magnitude. By using Eqs. (4) and (5) we include the influence of (the charge of) all the amino acids on the ionization degree of each titratable group via the smeared-out surface potential y_p . Via y_p also the dependence of ionic strength on α_i is included. However, local variations in potential over the protein surface, and a pertur-

bation in pK due to a (nonelectrostatic) influence of nearby amino acid residues is not considered in the model [16].

Electrostatic contribution to the thermodynamic functions

Solving the cell model analytically results in an expression for the electrostatic contribution to the osmotic pressure of the protein mixture, Π , given by [8]

$$\Pi_{el} = \frac{\kappa^2 b \lambda_B}{6v} \frac{1 - t_h^2}{(t_h + \kappa a)^2} \left[\frac{Q_1 Q_2}{\phi} \left(\sum_{i=1,2} \phi_i Z_i \right)^2 - \sum_{i=1,2} \phi_i Z_i^2 \right] \quad (6)$$

with

$$Q_2 = 2t_h(t_h + \kappa a) + 1 - t_h^2 + Q_1(t_h + \kappa a) \times \left[\frac{a}{\kappa b^2} + \frac{1}{\kappa^2 b^2} t_h - \left(\frac{1}{\kappa b} - \kappa a \right) (1 - t_h^2) \right], \quad (7)$$

irrespective of whether the colloids are charge regulating or not. The electric contribution to the potential, μ_{el} , remains unmodified as well [8]:

$$\mu_{i,el} = \frac{1}{2} Z_i y_i + \frac{1}{2} (Z_i - Z_j) \frac{Q_1 \kappa \lambda_B \phi_j}{\phi^2} \frac{1 - t_h^2}{t_h + \kappa a} \sum_{i=1,2} \phi_i Z_i + \Pi_{el} \frac{v}{\phi} \quad (8)$$

but for the charge-regulation model we must add to μ a chemical contribution because of the varying ionization degrees, given by [13,14,17,18]

$$\mu_{i,chem} = -Z_i y_i + \sum_j q_j \ln(1 - \alpha_j) \quad (9)$$

with the summation running over the six types of ionizable amino acid residues.

Nonelectrostatic contribution to the thermodynamic functions

The nonelectrostatic contributions are described using the Carnahan–Starling–van der Waals equation of state which gives as contribution to the osmotic pressure

$$\Pi_{nonel} v = \phi \frac{1 + \phi + \phi^2 - \phi^3}{(1 - \phi)^3} - \chi \phi^2, \quad (10)$$

and to the chemical potential

$$\mu_{i,nonel} = \ln \phi_i + \frac{\phi(8 - 9\phi + 3\phi^2)}{(1 - \phi)^3} - 2\chi\phi. \quad (11)$$

In the above equations, ϕ is the overall volume fraction of protein molecules and ϕ_i is the volume fraction of each individual component. A nonelectrostatic, temperature-dependent, attraction between the colloids is included via the parameter χ . Note that the attraction term and the volume exclusion term contain only the total protein concentration ϕ : we do not distinguish between the two types of molecules at this level. To describe phase separation in (one-component) protein solutions, the use of Eqs. (10) and (11)

was already proposed by Taratuta *et al.* [19] and Petsev *et al.* [20] We extend that approach to multicomponent protein solutions, and explicitly describe the electrostatic interactions (not, e.g., via a modification of the χ parameters).

At equilibrium, the osmotic pressure Π (combining electrostatic and nonelectrostatic contributions) is equal in both phases, as well as the potential μ for the two components. Finally, overall mass balances for the two protein molecules are required, such as Eq. (25) in Ref. [8].

Fixed number of small ions

In most of the calculations we will assume a fixed background ionic strength c_∞ , given by the amount of added salt. However, it turns out that in the experiments shown in Fig. 4 below this assumption fails below ~ 2 mM salt. Instead, we must consider that the number of ions in the system is fixed. As all experiments at low ionic strength were done at low pH values it was HCl that was used to adjust pH ; therefore it is the number of cations (N_a) that is fixed (i.e., not influenced by adjusting pH) and will be considered in the ion balances.

In the low-potential, Debye-Hückel, approach, the protein charge Z (let us assume it to be positive) is 50% compensated by a cation deficiency, and 50% by an excess of anions near the colloid (and vice versa for a negatively charged colloid). Thus, the total cation balance reads

$$n_{C,\text{added}} = n_\infty - \frac{1}{2v} \sum_j \zeta_j \sum_i \phi_{i,j} Z_{i,j}. \quad (12)$$

where n is the cation concentration, n_∞ the ionic strength used in the definition of the Debye length κ^{-1} , and ζ the relative volume of phase j ($0 < \zeta < 1$). In one calculation we will assume that q^* cations are codissolved with each protein molecule; in that case we must add to the left-hand side of Eq. (12) the term $+\phi_0 q^*/v$, where ϕ_0 is the total protein volume fraction.

Summary of input parameters required in the theory

To summarize, the theoretical model requires the following input parameters. First, for each protein type we need the number of each of the six types of ionizable groups, q_i , and the intrinsic pK value of each of them. Next, we need to assume a certain volume per molecule, v , and a certain value for the attraction parameter χ (which depends on temperature). Then we can make a calculation as a function of the overall volume fraction of each protein in the system ($\phi_{i,0}$, which gives us the overall mixing ratio α_0), pH , and Debye length κ^{-1} , the latter either directly based on the added salt concentration c_{salt} (n_∞), or indirectly via Eq. (12). The theory then predicts whether or not phase separation occurs, and if so, predicts the composition and density of each of the two phases. All parameters in the theory can be obtained from other sources: q_i follows directly from the amino acid composition of each protein, while pK values [21] and the protein volume [22] are obtained from the literature. We use the attraction parameter χ as a freely adjustable parameter

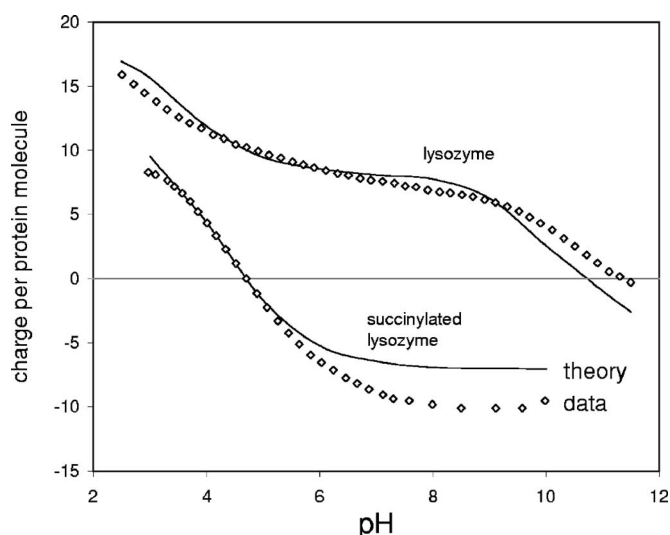


FIG. 1. Protein charge as function of pH for (succinylated) lysozyme ($c_\infty=50$ mM) [15,23].

though the range of values we use is comparable to those found for pure-lysozyme systems, as discussed in Ref. [8].

EXPERIMENT

Proteins

Succinylated lysozyme (SL) with molecular weight (MW_{SL}) 15.2 kDa is synthesized from hen egg white lysozyme (L; $MW_L=14.3$ kDa) by a procedure described in Ref. [23]. Subsequently it is dialyzed three times against a large excess of distilled water. For both molecules we use in the calculations a volume of $v=37$ nm³, as in Ref. [8]. The overall mixing ratio α_0 is the overall number concentration of L divided by the total protein number concentration, and, because the volume per molecule is assumed the same for L and SL, it is also equal to the volume fraction of L over the total volume fraction of L+SL [note that α is the ionization degree; see Eq. (5)]. We use the same titration model for L and SL as in Refs. [8] and [15] but note that in Ref. [8] the charge was calculated for a molecule in an infinitely dilute solution, using $t_h=1$ in Eq. (2), which in the present work will be done for calculations with the CC model only. In the CR model the charge per molecule is different in the dilute and complex phases.

Equations (4) and (5) require the intrinsic pK value of each of the amino acids, pK_i , and the number of each of these amino acids per protein molecule, q_i . For the anionic amino acids we use $pK_D=pK_E=4.4$ and $pK_Y=10$; for the cationic amino acids $pK_R=12$, $pK_H=6.5$ and $pK_K=10$ [21]. For lysozyme we have $q_D=7$, $q_E=2$, $q_Y=3$, $q_R=11$, $q_H=1$, $q_K=6$; for SL $q_D=16$, $q_E=2$, $q_Y=0$, $q_R=11$, $q_H=1$, and $q_K=0$. These values result in theoretical isoelectric points of $pI_L=10.7$ and $pI_{SL}=4.7$, respectively. For illustration purposes, we show in Fig. 1 the measured and calculated protein charge as a function of pH , for an ionic strength $c_\infty=50$ mM, taken from Refs. [15] and [23].

Phase separation

The protein molecules are dissolved in separate (one-component) stock solutions of a certain ionic strength

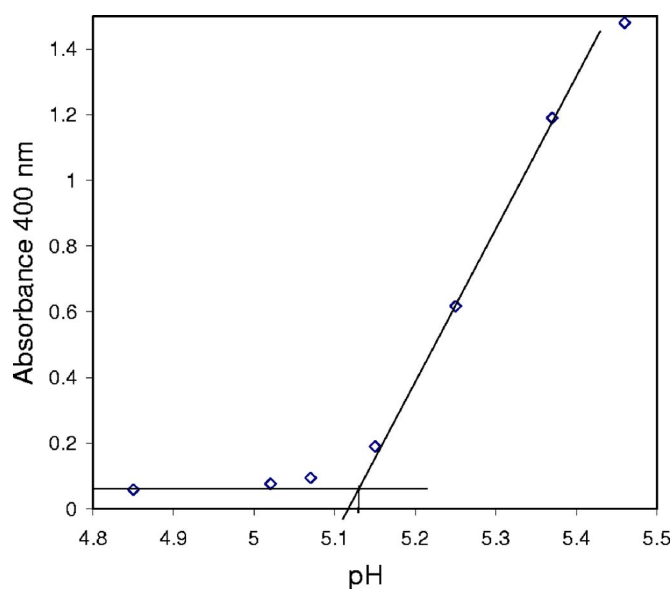


FIG. 2. (Color online) Typical example of method I to determine phase boundary from absorbance measurements ($\alpha_0=0.5$, $\phi_0=0.2$ vol %, no added salt, room temperature).

(NaCl), after which the solutions are mixed in certain proportions in a 25 ml stirred glass tube. We assume that the dialyzed and freeze-dried polymer is free of water and contaminants and will use the molar masses of the protein as given above to calculate the protein concentration and volume fraction (using $v=37$ nm³ per molecule). After each pH adjustment (with either HCl or NaOH) we wait for several minutes before taking a measurement. The following three methods were used to study phase separation in the mixed protein solutions:

METHOD I. Spectrophotometrically, the absorbance is measured at 400 nm (turbidity) as function of pH . To obtain the critical condition for the onset of phase separation a range of measurements is made at different pH values and the critical value pH_{crit} obtained from the construction illustrated in Fig. 2. This procedure is used for the data in Figs. 3 and 4 below.

METHOD II. Mixtures are transferred into capped plastic Eppendorf tubes of 1.5 ml, centrifuged for 30 min at 10 000 rotations/min, and left to equilibrate for 1 h, after which the protein concentration in the supernatant phase was determined spectrophotometrically (281.5 nm) using a calibration curve.

METHOD III. Mixtures are prepared, transferred into capped glass tubes (~ 3 ml), and placed in a stirred water bath. The temperature of the bath is increased slowly, ~ 0.2 °C/min, and we determine by eye at which temperature the sample becomes completely transparent, thus obtaining the clarification temperature $T_{clarify}$ [8,19,24]. Results of this method are plotted in Fig. 6 below.

RESULTS AND DISCUSSION

Method I: Turbidity experiments

In a first set of experiments we analyze phase behavior as a function of pH and composition, at a given protein concen-

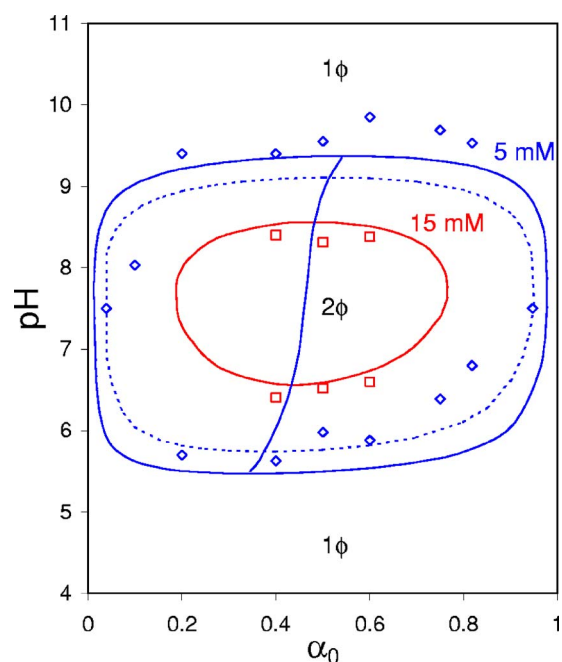


FIG. 3. (Color online) pH -composition phase diagram for lysozyme–succinylated lysozyme at 0.1 vol % total protein concentration at two values of the ionic strength (points denote onset of phase separation according to method I; see Fig. 2). Lines are based on the CR model (solid, $\chi=14$; dashed, $\chi=13$ and 5 mM). The almost vertical line gives for 5 mM salt and $\chi=14$ for each pH the mixing ratio α_0 at which the number of complexed molecules is at a maximum. 1ϕ denotes the one-phase, non-phase-separated, region; phase separation is observed in the 2ϕ region.

tration ($\phi_0=0.1$ vol %) and ionic strength (5 and 15 mM); see Fig. 3. A closed phase diagram is expected in the α_0 - pH plane because we can always move out of the two-phase “ 2ϕ ” region by increasing or decreasing pH or mixing ratio sufficiently. This is the case because at very low or very high pH all molecules have the same charge sign; and at increasingly asymmetric mixing ratios the system approaches a one-component system, which is for our conditions always stable (single-protein systems will phase separate when temperatures are very low and/or ionic strength or protein concentration is very high [19,30]). Indeed, a closed 2ϕ region is experimentally observed; see Fig. 3.

In addition, we expected the closed region to be tilted upward, with the pH window for phase separation shifted downward at a low mixing ratio α_0 , and upward at high α_0 , because, for instance, with decreasing pH the lysozyme molecules increase their charge and the SL molecules decrease their charge (in magnitude), and for charge neutrality in the complex we would then need more SL than L molecules, which suggests that the optimum mixing ratio shifts to lower amounts of L; thus the range of values of the mixing ratio α_0 for which phase separation occurs would decrease. However, though there certainly is an upward tilt in the experimental data, it is not very pronounced and for both low and high pH , we find a wide α_0 window around $\alpha_0=0.5$ where the pH for the onset of phase separation is rather independent of α_0 . The theoretical curves (based on the CR model) show an even slighter tilt.

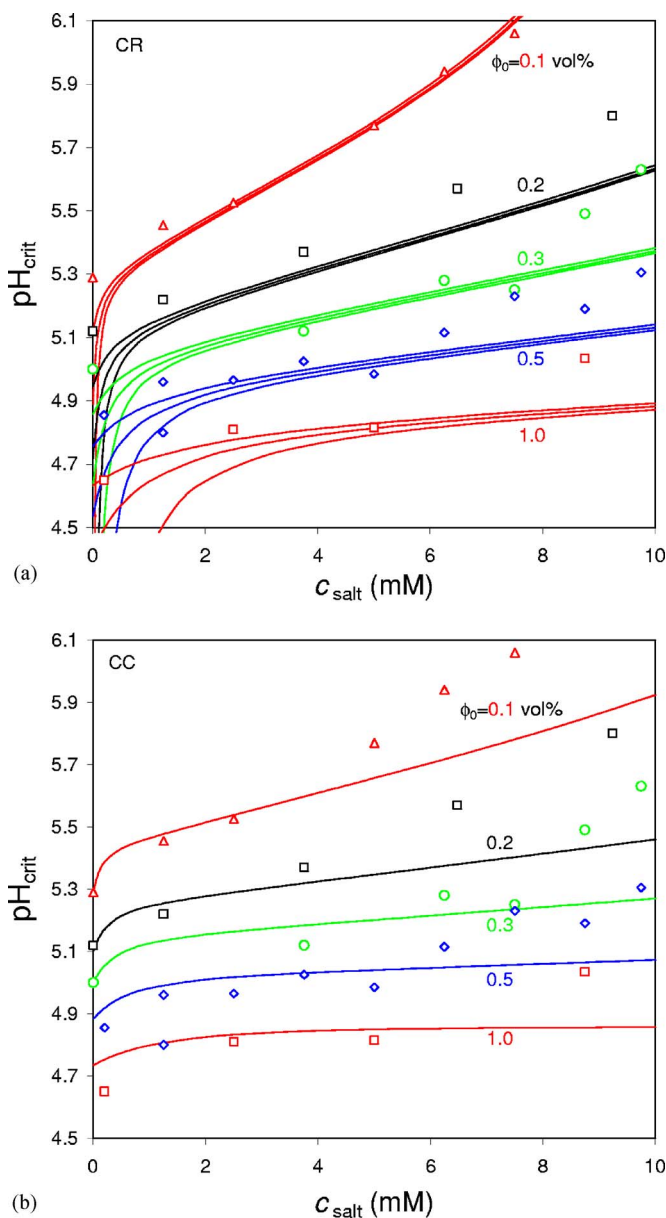


FIG. 4. (Color online) pH -added salt concentration phase diagram for lysozyme-succinylated lysozyme at 0.1 vol % total protein concentration at a symmetric mixing ratio, $\alpha_0=0.5$ (method I). Above each theoretical curve, or set of data points, the system is phase separated (a) CR model and (b) CC model. In (a) each set of three theoretical curves is based from bottom to top on fixed background ionic strength, fixed number of cations, and the same with an additional $q^*=2$ cations per protein molecule.

Now, because here, both theoretically and experimentally, only the *onset* of phase separation is reported, it might be interesting to investigate the conditions for maximum phase separation, and see if an upward tilt is perhaps observed in that parameter: if we increase pH , will the mixing ratio α_0 at which the complexed amount is at a maximum, $pH_{\max\text{compl}}$, steadily shift upward? The approximately vertical curve of $\alpha_{0,\max\text{compl}}-pH$ in Fig. 3 gives the result, and shows that although $\alpha_{0,\max\text{compl}}$ shifts upward with increasing pH , the effect is not very strong. Clearly, the intuitive idea that with

increasing pH the optimum condition for complexation shifts to higher relative concentrations of L, α_0 , is only slightly borne out by the experiments and theory.

The solid lines in Fig. 3 are based on the CR model and $\chi=14$ for a best fit to the data [$\chi=14$ is also the derived value in Fig. 6(b) for the CR model at room temperature, $T\sim 22^\circ\text{C}$]. We also plot our prediction for $\chi=13$ (dashed curve) as this is the best-fit value in the experiments shown later in Fig. 4. Though this value gives a reasonable prediction at 5 mM, at 15 mM absence of phase separation is predicted, in disagreement with the experimental observation. Calculations in Fig. 3 are all based on the CR model; the CC model predicts a somewhat less extended phase boundary in the vertical pH direction (not shown), and therefore describes the data somewhat less accurately.

In a next set of experiments the aim was to find a phase-separated system at a pH value as far away as possible from the optimum range around $pH 7.5$. We chose to lower pH toward the isoelectric point of succinylated lysozyme because this requires less addition of HCl than the required amount of NaOH addition in the case of going to the pI of lysozyme, ~ 11.5 . Experiments were done at a symmetric mixing ratio $\alpha_0=0.5$, because the analysis in Fig. 3 suggests that lowering α_0 does not expand the region of phase separation to lower pH very significantly. Second, we also decided to lower the ionic strength because a low ionic strength favors phase separation. Experimental results are shown in Fig. 4 together with three sets of calculations. In Fig. 4(a) we include charge regulation, optimize the χ value to $\chi=13$, and use three different ways to include the cations, namely, as follows. For each protein concentration ϕ_0 , the lowest curve is based on a calculation in which it is assumed that the ionic strength n_∞ is given by the added amount of salt. Though the data are rather well described down to ~ 2 mM salt, we find a clear deviation at lower ionic strengths. The theory predicts that upon lowering the ionic strength we will for all pH values ultimately end up in a phase-separated regime. The data, however, suggest that even without adding salt still a distinct critical pH value is found below which the system is a single phase (no complex phase formed). Therefore we include in the calculation the fact that the number of cations is finite, by using Eq. (12), which results in the middle curves in Fig. 4(a). This adjustment already gives a significantly improved result, with at 0 mM added salt finite values for pH_{crit} predicted, in line with the data. However, the predicted values for pH_{crit} are still too low. A final modification to the theory is to include the possibility that with each protein molecule $q^*=2$ cations are codissolved. Interestingly, this modification brings the theoretical prediction rather close to the experimental data [see each of the upper curves in Fig. 4(a)] which suggests that, despite dialysis, a small number of ions is retained in the protein sample. This is not unlikely as also during dialysis the protein molecules tend to remain charged, which requires counterions to remain nearby. Only ion exchange, or dialysis against an extremely ion-free dialyzing fluid, will result in an essentially ion-free protein sample.

Of the data in Fig. 4, one data point is at a pH value around the isoelectric point of succinylated lysozyme (namely, at the highest protein concentration of 1 vol %, at

0.2 mM salt), which was the lowest pH_{crit} we could obtain. At higher protein concentrations we did not obtain a suitable turbidity data set such as shown in Fig. 2, but instead upon lowering pH to values below pH 4.5 we found that the turbidity increased rapidly again. After that, the sample remained turbid at all pH values (not reversible). It seems that at these low pH values and high protein concentrations there is a nonreversible attraction, not accounted for in the current theoretical approach, perhaps related to some protein unfolding. Therefore we will leave these conditions out of the present analysis.

A second use of the data set of Fig. 4 is to compare the predictive power of the CR model, Fig. 4(a), with that of the CC model, Fig. 4(b). To that end, we fitted in panel Fig. 4(b) the CC model to the data, making use of the same assumptions with respect to the small ions as in the best fit for panel *a* (namely, taking account of the finite number of cations, and with $q^*=2$), and separately fit the attraction strength χ ($\chi_{CC}=14.5$). We find that the CR model gives a somewhat better prediction of the phase boundary than the CC model, the most notable difference being that the theoretical curves in Fig. 4(b) (CC model) are almost horizontal, in contrast to both the experiments and to the theoretical curves in Fig. 4(a) (CR model) where the model predicts a positive slope which rather closely matches the experiment. This comparison of CC and CR models suggests that indeed the molecules do adjust their charge to the local proton concentration when moving from the complex phase to the supernatant and vice versa.

Method II: Centrifugation experiments

In a next set of experiments, again at room temperature, we do not measure the phase boundary (onset of phase separation) but instead the total amount of molecules in the complex phase, or alternatively, see Fig. 5, the percentage of molecules remaining in solution after centrifuging off the complex phase, ϕ_s/ϕ_0 (where ϕ_s is the supernatant concentration, and ϕ_0 the overall concentration). To convert the data (for absorbance at 281.5 nm) to ϕ_s/ϕ_0 , we rescale each data set such that at low pH ϕ_s/ϕ_0 equals 100%. Figure 5 presents data and theory for ϕ_s/ϕ_0 as a function of pH and ionic strength. Data and theory both show that at extreme enough pH we have a stable system (single phase, 100% in solution) whereas a dip in ϕ_s/ϕ_0 develops at intermediate pH . The dip expands to a wider pH range and increases in depth with decreasing ionic strength, in both theory and the experiments. With a fitted value of $\chi=13$ the theory describes the three datasets best, and also predicts the minimum value of the supernatant concentration for each ionic strength reasonably well. However, there are significant deviations too: the change of ϕ_s/ϕ_0 with ionic strength is overestimated, and the extent of complexation at higher pH (beyond $pH \sim 8.5$) is significantly overestimated. This latter effect might well be due to the fact that the titration model, which is rather accurate for $4 < pH < 6$ for both molecules (see Fig. 1), starts to deviate from the data at $pH > 8$. A better titration model [16] might improve the quality of the model in this pH range. Using a slightly lower χ (namely, $\chi=12.5$) significantly im-

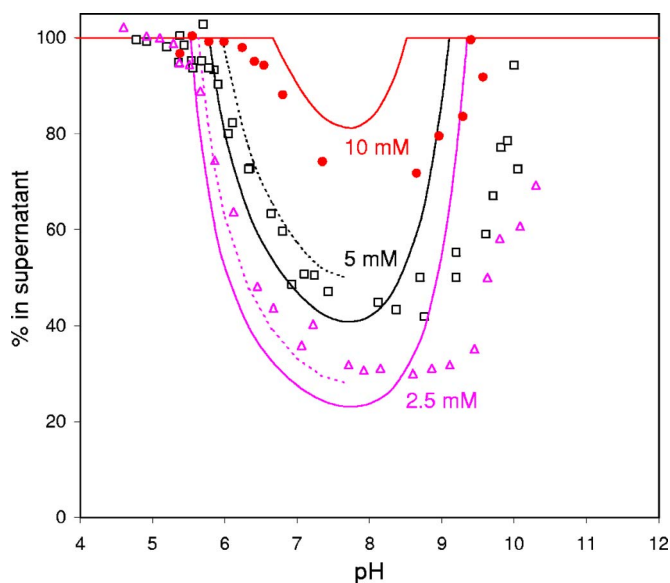


FIG. 5. (Color online) Percentage of total protein remaining in supernatant phase as function of pH and ionic strength ($\phi_0 = 0.1$ vol %, $\alpha_0 = 0.5$, method II). Theoretical curves based on the CR model with $\chi=13$ (dashed curves $\chi=12.5$).

proves the fit for 2.5 and 5 mM salt for $pH < 8$ (dashed lines in Fig. 5) but would, over the entire range of pH and ionic strength, not be an overall improvement.

Method III: Temperature influence

Finally, we determined the clarification temperature of a phase-separated, turbid sample by increasing the temperature slowly, similar to the approach in Refs. [8,19,24], for a variety of values of pH and total protein concentration (mixing ratio $\alpha_0 = 0.5$; ionic strength = 5 mM). Subsequently, we used the same procedure as in Ref. [8], namely, to plot theoretical χ values for the onset of phase separation at each experimental condition (pH , ionic strength, etc.) against the experimental temperature. If the theory is valid, a single $\chi(T)$ curve should describe the data; if not, the various points will be scattered across space. We performed this procedure to see, first of all, if the theory is able to describe the experiment also for asymmetric charge ratios, and second, if we can distinguish between the CC model and the CR model in their predictive power. Results are presented in Fig. 6. We see that with both models a well-defined $\chi(T)$ correlation is found, with about the same extent of scatter around the best-fit curve. In both cases, the scatter in the data is much larger below 15 °C than at higher temperatures. Indeed, at low temperature it was more difficult to ascertain experimentally whether or not the sample had become completely transparent; at higher temperatures the transition from turbid to transparent was more distinct (i.e., occurred over a smaller temperature interval).

The predictive power of both models can best be compared for the three data sets at pH 5.4, 5.6, and 6.0 (at pH 5.0, 5.2, and 5.8 the models cannot be distinguished in their predictive power). Making this analysis we see that the CR model (full curves) gives a somewhat better prediction than

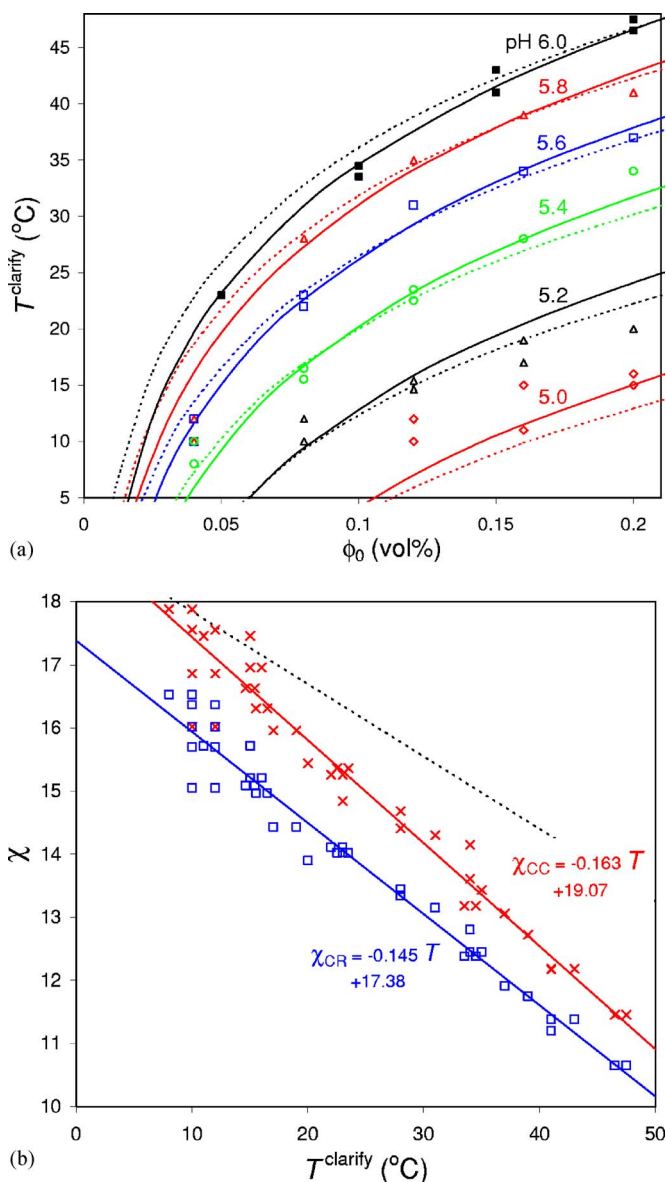


FIG. 6. (Color online) (a) Clarification temperature as function of pH and total protein concentration, ϕ_0 ($\alpha_0=0.5$; $c_{\text{salt}}=5$ mM). Solid lines show calculation results for the charge regulation, CR, model and dashed lines for a fixed protein charge (CC model). (b) $\chi(T)$ correlation for the CC (crosses) and CR models (squares). Also shown (dashed line) is the $\chi(T)$ correlation from Ref. [8].

the CC model (dashed lines). Thus, very tentatively, also this set of experiments suggests that the protein molecules do indeed charge regulate, and adjust their charge when moving into and out of the dense phase.

Discussion of nonelectrostatic attractive force

Though the theory reasonably well describes the data of protein phase separation, at least two problems remain. First of all, the fact that different numerical values for χ have to be used throughout this work, as well as in Ref. [8], and secondly that the origin (of the temperature dependence) of the attractive force is not very well known.

On the first point, it must be remarked that when we jointly consider the various data sets in this paper together with those in Ref. [8], it is not possible to use a single value for χ , but different values need to be used for the different experimental protocols (even when using the same method). For instance, the best-fit values for χ are different in Figs. 3 and 4, while there is also a difference in the $\chi(T)$ -curve [see Fig. 6(b)], between the experiments in this paper (5 mM salt, pH 5.0–6.0) and those in Ref. [8] (5–40 mM, pH 7.5). This shows that the theoretical model is certainly still insufficient in describing the underlying forces in this system accurately.

To improve the model, and possibly to describe the temperature dependence to some extent, one could consider the following aspects. One cause for the influence of temperature on the 2ϕ stability is possibly a decrease in protein charge with increasing temperature via an influence on the pK values. However, Schaller and Robertson [25] conclude from their study on turkey ovomucoid third domain (a protein) that “no significant changes in pK_a were observed over the 25 °C temperature change employed... which leads us to conclude that none of the apparent ionization enthalpies ΔH_{ion} exceeds 2 kcal/mol.” For sperm whale metmyoglobin, Breslow and Gurd [26] find ΔH_{ion} ranging from 2.5 kcal/mol for the carboxylic groups to 10.7 kcal/mol for the amine groups. Using $\partial pK/dT = -\Delta H_{\text{ion}}/(\ln 10)RT^2$ (with ΔH_{ion} in J/mol and R the gas constant) [26,27] and using $T = 300$ K, we calculate that these values for ΔH_{ion} result in a pK decrease [13] of 0.15 to 0.65 over a 25 °C temperature range (similar data for ΔH_{ion} are in Ref. [28]). Indeed these values are not very large and will not readily result in the observed significant effect of temperature on complexation behavior. Another effect of temperature on the electrostatic interaction is via the permittivity ϵ of water. However, ϵT , which is the relevant parameter that shows up in the Debye length, only varies very weakly with temperature [29] (3% over 25 °C; thus κ only changes by 1.5%). A final suggestion for an electrostatic origin of the attraction and its temperature dependence is that due to the inhomogeneous charge distribution over the surface of the protein molecules a dipolar attraction develops with a positive patch on one molecule orienting toward a negative patch on the next. At higher temperature, with increasing thermal energy, the tendency of the protein molecules to diffuse and rotate increases (a larger force would be necessary to keep them locked in, without rotating), and therefore the dipolar attraction might be significantly reduced. At this point we have no means to quantify the strength of a possible dipolar attraction.

However, most probably the attractive term, and its temperature dependence, “which can hardly be reconciled with a purely electrostatic approach” [30] have a chemical origin related to nonelectrostatic (solvation, hydrophobic) interactions. Chemical modification of proteins is a known method to increase hydrophobicity, which is, e.g., used to compare native and modified proteins in adsorption experiments [31,32]. Our succinylated lysozyme is most likely more hydrophobic than (native) lysozyme, resulting in increased hydrophobic interactions. Possibly also a nonelectrostatic effect related to (solvation of) the small ions can contribute to this attractive term [33]. We have attempted in the present work to separate out the mean-field electrostatic forces and volume

and entropy effects from this attractive protein-protein interaction “[of which] the molecular origins are poorly understood” [33] and to empirically quantify its strength and temperature dependence.

CONCLUSIONS

Mixtures of lysozyme and succinylated lysozyme phase separate under suitable conditions: low ionic strength, low temperature, symmetric mixing ratio, high protein concentration, and pH near to conditions when they both have high, opposite, charge, thus ideally around pH 7.5. Moving away from optimal conditions, fewer and fewer molecules remain in the complex phase, and ultimately phase separation ceases. A thermodynamical model based on a heterogeneous cell model for the electrostatic interactions describes the experimental data well, also at asymmetric charge ratios.

A theoretical model that includes charge regulation gives a somewhat better fit to the data than in case a fixed charge is

assumed, which suggests that the protonation reactions that determine the charge of a protein molecule are sufficiently fast compared to the rate of protein exchange between supernatant and complex phase. For ionic strengths below 2 mM and at protein concentrations of 0.1 vol% (~ 1 g/l) a constant background ionic strength (given by the amount of added salt) can no longer be assumed, but instead we must consider that the number of cations and anions in the system is fixed, as well as that the dialyzed and dried protein samples contain a small number of cations (~ 2 per protein molecule). A temperature-dependent nonelectrostatic attractive term is required to bring the model into quantitative agreement with the data.

ACKNOWLEDGMENTS

This research was financially supported by NWO, Netherlands Organization for Scientific Research, and the Alexander von Humboldt Foundation, Germany.

-
- [1] A. van Blaaderen, *Nature (London)* **439**, 545 (2006).
 [2] D. Frenkel, *Nat. Mater.* **5**, 85 (2006).
 [3] W. Lin, M. Kobayashi, M. Skarba, C. Mu, P. Galletto, and M. Borkovec, *Langmuir* **22**, 1038 (2006).
 [4] M. E. Leunissen, C. G. Christova, A. P. Hynninen, C. P. Royall, A. I. Campbell, A. Imhof, M. Dijkstra, R. van Roij, and A. van Blaaderen, *Nature (London)* **437**, 235 (2005).
 [5] F. N. Braun, S. Paulsen, R. P. Sear, and P. B. Warren, *Phys. Rev. Lett.* **94**, 178105 (2005).
 [6] P. Bartlett and A. I. Campbell, *Phys. Rev. Lett.* **95**, 128302 (2005).
 [7] M. Raša, A. P. Philipse, and J. D. Meeldijk, *J. Colloid Interface Sci.* **278**, 115 (2004).
 [8] P. M. Biesheuvel, S. Lindhoud, R. de Vries, and M. A. Cohen Stuart, *Langmuir* **22**, 1291 (2006).
 [9] J. Liu and E. Luijten, *Phys. Rev. Lett.* **93**, 247802 (2004).
 [10] J. B. Caballero, A. M. Puertas, A. Fernández-Barbero, and F. J. de las Nieves, *J. Chem. Phys.* **121**, 2428 (2004).
 [11] P. M. Biesheuvel and M. A. Cohen Stuart, *Langmuir* **20**, 4764 (2004).
 [12] D. Stigter and K. A. Dill, *Biochemistry* **29**, 1262 (1999).
 [13] D. Stigter, D. O. V. Alonso, and K. A. Dill, *Proc. Natl. Acad. Sci. U.S.A.* **88**, 4176 (1991).
 [14] D. O. V. Alonso, K. A. Dill, and D. Stigter, *Biopolymers* **31**, 1631 (1991).
 [15] P. M. Biesheuvel, M. van der Veen, and W. Norde, *J. Phys. Chem. B* **109**, 4172 (2005).
 [16] D. E. Kuehner, J. Engmann, F. Fergg, M. Wernick, H. W. Blanch, and J. M. Prausnitz, *J. Phys. Chem. B* **103**, 1368 (1999).
 [17] P. M. Biesheuvel, *Eur. Phys. J. E* **16**, 353 (2005).
 [18] P. M. Biesheuvel and A. Wittemann, *J. Phys. Chem. B* **109**, 4209 (2005).
 [19] V. G. Taratuta, A. Holschbach, G. M. Thurston, D. Blank-schtein, and G. B. Benedek, *J. Phys. Chem.* **94**, 2140 (1990).
 [20] D. N. Petsev, X. Wu, O. Galkin, and P. G. Vekilov, *J. Phys. Chem. B* **107**, 3921 (2003).
 [21] L. Stryer, *Biochemistry* (Freeman, New York, 1995).
 [22] F. L. González Flecha and V. Levi, *Biochem. Mol. Biol. Educ.* **31**, 319 (2003).
 [23] M. van der Veen, W. Norde, and M. A. Cohen Stuart, *Colloids Surf. B* **35**, 33 (2004).
 [24] C. Liu, N. Asherie, A. Lomakin, J. Pande, O. Ogun, and G. B. Benedek, *Proc. Natl. Acad. Sci. U.S.A.* **93**, 377 (1996).
 [25] W. Schaller and A. D. Robertson, *Biochemistry* **34**, 4174 (1995).
 [26] E. Breslow and F. R. N. Gurd, *J. Biol. Chem.* **237**, 371 (1962).
 [27] R. W. Ramette, *J. Chem. Educ.* **54**, 280 (1977).
 [28] M. Tanaka, H. Nomura, and F. Kawaizumi, *Bull. Chem. Soc. Jpn.* **65**, 410 (1992).
 [29] B. B. Owen, R. C. Miller, C. E. Milner, and H. L. Cogan, *J. Phys. Chem.* **65**, 2065 (1961).
 [30] R. Piazza, *Curr. Opin. Colloid Interface Sci.* **8**, 515 (2004).
 [31] S. Magdassi, A. Kamyshny, and A. Baszkin, *J. Dispersion Sci. Technol.* **22**, 313 (2001).
 [32] P. A. Wierenga, M. B. J. Meinders, M. R. Egmond, F. Voragen, and H. H. J. de Jongh, *Langmuir* **19**, 8964 (2003).
 [33] R. A. Curtis and L. Lue, *Chem. Eng. Sci.* **61**, 907 (2006).